A quantum cascade laser infrared spectrometer for CO2 stable isotope analysis: Field implementation at a hydrocarbon contaminated site under bio-remediation

Christophe Guimbaud, Cécile Noel, Michel Chartier, Valéry Catoire, Michaela Blessing, Jean Christophe Gourry, C Robert

JOURNAL OF ENVIRONMENTAL SCIENCES 40 (2016) 60–74

Available online at www.sciencedirect.com

ScienceDirect

www.elsevier.com/locate/jes

JES JOURNAL OF ENVIRONMENTAL SCIENCES

www.jesc.ac.cn

A quantum cascade laser infrared spectrometer for CO_2 stable isotope analysis: Field implementation at a hydrocarbon contaminated site under bio-remediation

Christophe Guimbaud[1,*], *Cécile Noel*[1,2], *Michel Chartier*[1], *Valéry Catoire*[1], *Michaela Blessing*[2], *Jean Christophe Gourry*[2], *Claude Robert*[1]

1. *Laboratoire de Physique et de Chimie de l'Environnement et de l'Espace (LPC2E), CNRS et Université d'Orléans (UMR 7328), 45071 Orléans cedex 2, France*
2. *Bureau de Recherches Géologiques et Minières (BRGM), 45060 Orléans cedex 2, France*

ARTICLE INFO

Article history:
Received 28 July 2015
Revised 7 October 2015
Accepted 27 November 2015
Available online 8 January 2016

Keywords:
Isotope ratio infrared spectrometry
Isotopic signature $\delta^{13}C$ of CO_2
Biodegradation monitoring
Hydrocarbons
BTEX

ABSTRACT

Real-time methods to monitor stable isotope ratios of CO_2 are needed to identify biogeochemical origins of CO_2 emissions from the soil–air interface. An isotope ratio infra-red spectrometer (IRIS) has been developed to measure CO_2 mixing ratio with $\delta^{13}C$ isotopic signature, in addition to mixing ratios of other greenhouse gases (CH_4, N_2O). The original aspects of the instrument as well as its precision and accuracy for the determination of the isotopic signature $\delta^{13}C$ of CO_2 are discussed. A first application to biodegradation of hydrocarbons is presented, tested on a hydrocarbon contaminated site under aerobic bio-treatment. CO_2 flux measurements using closed chamber method is combined with the determination of the isotopic signature $\delta^{13}C$ of the CO_2 emission to propose a non-intrusive method to monitor *in situ* biodegradation of hydrocarbons. In the contaminated area, high CO_2 emissions have been measured with an isotopic signature $\delta^{13}C$ suggesting that CO_2 comes from petroleum hydrocarbon biodegradation. This first field implementation shows that rapid and accurate measurement of isotopic signature of CO_2 emissions is particularly useful in assessing the contribution of contaminant degradation to the measured CO_2 efflux and is promising as a monitoring tool for aerobic bio-treatment.

Introduction

Flux measurement of CO_2 from land-air interface with $\delta^{13}C/^{12}C$ (labeled $\delta^{13}C$) characterization allows a better understanding of the biogeochemical mechanisms of the C cycle leading to the CO_2 emissions (Ghosh and Brand, 2003). Biogeochemical processes as photosynthesis, photorespiration, and soil microbial respiration come with isotopic fractionation of $\delta^{13}C/^{12}C$ of the carbon atom (Schweizer et al., 1999; Ekblad and Högberg, 2000; Gilbert et al., 2011).

Real-time methods to monitor stable isotope ratios of CO_2 are thus needed to improve our understanding of its sources and sinks (Nelson et al., 2008, and references therein). The characterization of the biogeochemical origins of CO_2 emissions from land–air interface may need a precision as good as 10^{-4} (or 0.1‰) for the determination of the isotopic signature $\delta^{13}C$ of

* *Corresponding author*. E-mail: christophe.guimbaud@cnrs-orleans.fr (Christophe Guimbaud).

http://dx.doi.org/10.1016/j.jes.2015.11.015
1001-0742/

CO_2. IRMS (isotope ratio mass spectrometry) commonly is the standard method for isotopic abundance analysis because of its high precision (<0.1‰). However IRMS is not suitable for real-time continuous analysis or for field deployment. Many studies have now shown that IRIS (isotope ratio infra-red spectrometry) can reach this suitability, with a better mobility and a precision which gets closer to IRMS, as shown by the IRIS instruments being developed and tested in the field (Bowling et al., 2005; Schaeffer et al., 2008; Croizé et al., 2008; Nelson et al., 2008; Richter et al., 2009).

For the investigation of the biogeochemical origins of CO_2 emissions from land–air interface, LPC2E has developed an IRIS instrument, SPIRIT (spectrometer infra-red *in situ* tropospheric), to measure CO_2 flux with $\delta^{13}C$ isotopic signature, in addition to the measurement of fluxes of other greenhouse gases (GHG), such as CH_4 and N_2O previously described (Guimbaud et al., 2011; Grossel et al., 2014).

The goal of our development is not to reach better performances of IRIS instruments described above but to keep the versatility of SPIRIT for different species analysis. The objective is to keep the easy length path modulation of the original large volume cell of SPIRIT to switch from CO_2 to CH_4/N_2O ambient air analysis with the capacity to characterize the $\delta^{13}C$ isotopic signature of CO_2 with a precision high enough for geochemistry applications. As a consequence, other species isotopic ratios of biogeochemical interest such as $\delta^{13}C$ and $\delta^{2}H/^{1}H$ of CH_4 (Whiticar, 1999; Tsuji et al., 2006; Hornibrook and Bowes, 2007; Witinski et al., 2011) could be explored in the future as SPIRIT is versatile for both easy length path modulation and laser change. Therefore, long optical path is still preferred for N_2O and CH_4 analysis ability by keeping the SPIRIT large original volume cell and mirror diameter which provide a large number of stable reflections. Cell temperature regulation and thus the isotope ratio precision (strongly temperature dependent) are shown to be close to performances obtained from smaller volume optical cells ($\ll$1 L) commonly used from previous authors.

The original aspects of the instrument as well as its precision and accuracy for the determination of the isotopic signature $\delta^{13}C$ of the CO_2 are largely discussed. Precision for the determination of the isotopic signature $\delta^{18}O/^{16}O$ (labeled $\delta^{18}O$) of CO_2 is also given for information despite no standard calibration is used to check its accuracy. First original results applied to biodegradation of hydrocarbons are presented, tested on a hydrocarbon polluted site under aerobic bio-treatment. CO_2 flux measurement using closed chamber method is combined with the determination of the isotopic signature $\delta^{13}C$ of the CO_2 emission to propose a non-intrusive method for monitoring *in situ* biodegradation of hydrocarbons.

1. Instrument description

1.1. Modified version of SPIRIT

1.1.1. Implementation of an additional laser for CO_2 mixing ratio and $\delta^{13}C$ isotopic signature determination

SPIRIT (spectrometer infra-red *in situ* tropospheric), is a portable wheel infra-red spectrometer (~100 kg; 120 cm × 80 cm × 50 cm) developed by our group (Guimbaud et al., 2011) to measure gas phase volume mixing ratios of CH_4, N_2O and CO_2, as well as isotopic ratios of $^{13}C/^{12}C$ and $^{18}O/^{16}O$ of CO_2, as described in this paper.

SPIRIT is equipped with a patented non-resonant multi-pass optical cell (French patent FR2889599 and international patents WO 2007/017,570 A1; Robert, 2007) allowing for an easy length path modulation (*e.g.*, 14 to 84 m) to switch from CH_4/N_2O to CO_2 ambient air analysis, thanks to the rotation of one half of a broad band spherical mirror. Distributive feedback (DFB) quantum cascade laser (QCL) in continuous wave (CW) operates near room temperature (RT) in the mid IR region. These lasers emit a more considerable light power with better spectral resolution (10^{-4}/cm) than the classical lead-salt diode lasers and operate near ambient temperature.

SPIRIT is able to operate with three QCLs while keeping the use of one optical cell and two detectors, one for the measurement channel and one for the reference channel (with a Fabry Perot etalon for relative wavenumber calibration). The three lasers can work sequentially, triggered and synchronized by the data acquisition system within a periodicity of 1.5 sec, thanks to the home-made QCL emission controller.

The first version of SPIRIT operated with one laser only using the N_2O and CH_4 ro-vibrational lines positioned at the central wavenumbers 1261.9874 and 1262.2285/cm, with line intensities of 1.044×10^{-19} and 2.723×10^{-20} cm/molecule at 296 K, respectively (Rothman et al., 2009). The instrument description and method for CH_4 and N_2O concentration retrieval are reported in Guimbaud et al. (2011). SPIRIT has demonstrated high precision for CH_4 and N_2O mixing ratio measurement in ambient air (0.2% for 1.5 sec of integration time, namely ~4 ppb for CH_4 at 1.9 ppmV and ~0.6 ppb for N_2O at 320 ppbV) as well as for flux emission measurements above peatlands, lakes, and cultivated fields, using the closed chamber method (Guimbaud et al., 2011; Gogo et al., 2011).

A second laser has been implemented, using the $^{12}C^{16}O^{16}O$, $^{12}C^{18}O^{16}O$ and $^{13}C^{16}O^{16}O$ ro-vibrational lines positioned at the central wavenumbers 2310.0025, 2310.2056 and 2310.3470/cm, with line intensities of 4.664×10^{-21}, 4.637×10^{-21} and 6.447×10^{-21} cm/molecule, respectively (Rothman et al., 2005, 2009), as shown in Fig. 1.

1.1.2. Temperature regulated multipass cell for accurate $\delta^{13}C$ isotopic signature determination

For the identification of the biogeochemical origins of CO_2 emissions from land–air interface, the isotopic signature of CO_2 emissions is defined as $\delta^{13}C_{sample}$ (‰) or δ:

$$\delta = (R/R_{VPDB} - 1) \times 1000 \quad (1)$$

where, R and R_{VPDB} are the isotopic concentration ratios $^{13}C/^{12}C$ of the sample and of the international standard, the Vienna Pee Dee Belemnite, respectively. R_{VPDB} is 1.12372%, as defined by Craig (1954).

Ro-vibrational line strengths, mainly for $^{12}C^{16}O^{16}O$, are strongly temperature dependent. As a consequence, $\delta^{13}C$ isotopic signature of CO_2 precision is strongly dependent on temperature stability and precision and would require small volume optical cells ($\ll$1 L) for a better temperature regulation. However, due to the aim of the new SPIRIT instrument to measure mixing ratios of various atmospheric trace gases over

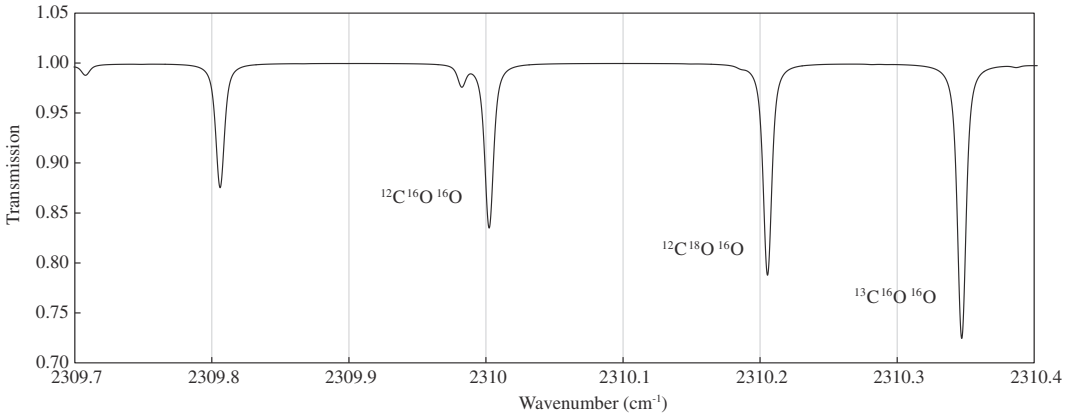

Fig. 1 – Transmission spectrum of CO_2 (400 ppmV in air) obtained from the Hitran database (Rothman et al., 2005, 2009) simulated at 30 hPa and 282 K at SPIRIT (spectrometer infra-red *in situ* tropospheric) resolution of 10^{-3}/cm.

a wide range of mixing ratios, it is decided to keep the same cell volume (3.3 L) and length (65 cm) with its easy length path modulation to switch from CO_2 to CH_4/N_2O ambient air analysis. Despite the fact that a larger volume cell is not optimized for fast temperature regulation, it provides good latent heat and the smoothest efficient temperature changes from the entering gas flow.

The multipass cell is reconstructed in aluminum alloy and stabilized at a temperature above ambient temperature by heating with a precision of ±0.02°C. The set value of this stabilized temperature system is specified at the start with the value of the optical bench temperature plus 5°C to reduce the heat loss. The cell is also covered with a thermal protection to reduce these heat loss and temperature gradient apart the cell. The multipass cell uses five feedback loop controls. These controls are located on points with heat flow. Each feedback control is built with a series of heating resistors and one temperature sensor (platinum resistor PT1000, JUMO GmbH, Fulda, Germany). Fig. 2 shows the distribution of these feedback loop controls. The heating resistors are thin flexible resistors (Minco, Fridley, Minnesota, USA). They are glued on the surface of the cell. The surface of each resistor is maximal to avoid heat point. The casings of the resistor cells are made of aluminum alloy for a good thermal conductivity. The first control (resistors H1 and the sensor T1) stabilizes the temperature of the front of the cell where it is fastened onto the optical bench. This control reduces the impact of the heat flow of the holding parts. The third control (H3, T3) performs the same role. The second control (H2, T2) reduces the heat leak of the long tube. To reduce the impact of air inlet we have two controls: H4, T4 and H5, T5. Each heating system is mounted with heater fins. This stabilizes the air temperature at the good value in the cell. We study all the feedback loop control to determinate the proportional integral derivative (PID) controllers and their interactions. Each controller impacts the stability of the others. These feedback controls are simulated with Matlab Simulink (MathWorks, Natick, Massachusetts, USA) software.

All temperature sensors (PT1000) of the cell are calibrated together in a climatic chamber. For a very good precision, the measures of the PT1000 are made with 4 wires. The calibration of these sensors has allowed the determination of correction function for each sensor with a precision of ±0.015°C in the range of 10–40°C. The PID controllers have an error close to zero thanks to the integral. Thus, the errors of all the controllers are essentially the errors of the measurement of the temperature.

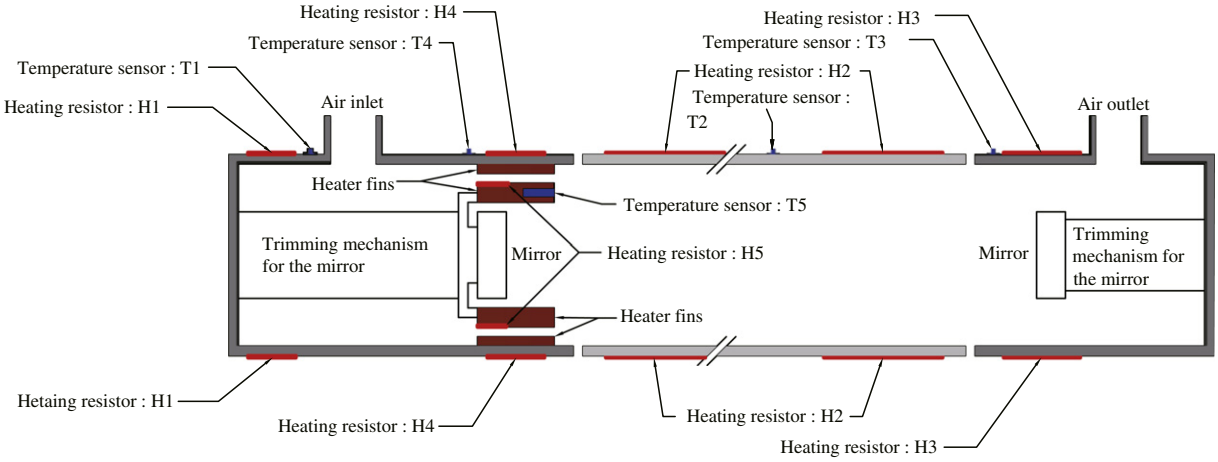

Fig. 2 – Sketch of the temperature control of the multipass cell.

1.1.3. Schematic design of the instrument

The method for concentration retrieval and the principle of the instrument were extensively described in Guimbaud et al. (2011). In Fig. 3, the main changes are schematized with the implementation of a temperature regulation for the multipass cell and the addition of two electro valves on the gas line at the input and at the output of the multipass cell.

This electro valves switch sequence allows for successive, isotopic calibration, sampling air isotopic monitoring (air sample in the atmosphere or in the accumulation chamber), and isotopic calibration again, for accurate $\delta^{13}C$ measurement and validation of air sample. The two electro valves are simultaneously switched from calibration gas input/output positions to air input/output positions (Fig. 3) for the measurement in the absorption cell of either calibration gas or air sample. The isotopic signature measurement, *i.e.*, $\delta^{13}C$ or $\delta^{18}O$ of CO_2 is made in three successive steps. First, the calibration gas coming from a compressed synthetic air cylinder is sent into the cell and the retrieved concentrations of each isotope are averaged over few minutes. These values are used in the next steps to establish isotopic signatures of the sample. Second, the two electro valves are simultaneously switched on and air sampling passes through the cell and isotope concentrations are measured. As the isotopic signature of the calibration gas is known, the isotopic signature of CO_2 in the sampled air is established according to calculations described later. Third, the electro valves are simultaneously switched back to the initial position and isotopic signature of the calibration gas is checked being equal to the reference value and then recalculated in the same way as previously described. This third step allows the determination of any drift of the instrument during this three step process and calibration is always performed again just before the next ambient air analysis.

1.1.4. Calculation of the isotopic signature $\delta^{13}C$ of CO_2

The isotopic signature of CO_2 in the air sampling measured with SPIRIT, defined as $\delta^{13}C$ or δ, is calculated from the measured ratios of the concentrations (^{13}C and ^{12}C) of each isotope of CO_2, *i.e.*,

$R = {}^{13}C/{}^{12}C$ (derived from analysis of ambient air)

and

$R^0 = {}^{13}C^0/{}^{12}C^0$ (derived from analysis of a reference synthetic compressed CO_2/air cylinders having typically a volume of 20 L and a pressure of 200 bar).

The reference cylinder is certified by Air Liquide (Centre-Bourgogne, France) in CO_2 volume mixing ratio, X^0, expressed in parts per million by volume (ppmV) and certified in isotopic signature $\delta^{13}C = \delta^0$ by gas bench isotope ratio mass spectrometry (gas bench-IRMS, Finnigan Gas Bench II, Thermo

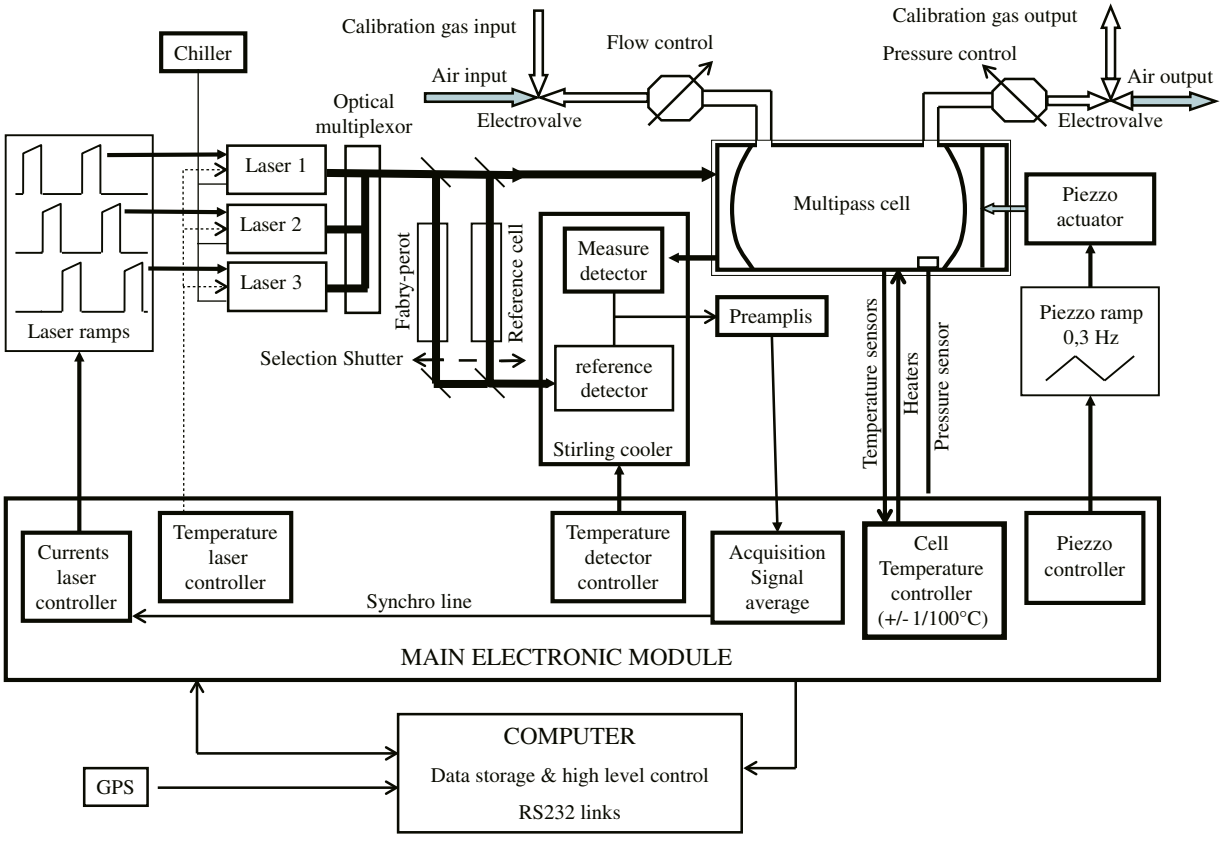

Fig. 3 – Schematic of the instrument design. GPS: global positioning system; RS232: standard computer port for serial communication transmission of data.

Electron Corporation, Bremen, Germany). Three consecutive reference cylinders (C1, C2 and C3) have been used:

C1 with X^0 = 407 ppmV and δ^0 = −40.53‰ ± 0.63‰ VPDB until January 2014.

C2 with X^0 = 390 ppmV and δ^0 = −43.24‰ ± 0.28‰ VPDB between February and July 2014

C3 with X^0 = 406 ppmV and δ^0 = −43.20‰ ± 0.42‰ VPDB since August 2014.

One of the previous δ^0 values, given by $(R^0 / R_{VPDB} - 1) \times 1000$ according to Eq. (1), is the one used for instrument calibration and then to calculate δ of sampling air. δ is by definition expressed *versus* VPDB, and we do not have access to the ratio of the calculated concentrations of each C isotope from the VPDB standard ($R_{VPDB} = (^{13}C/^{12}C)_{VPDB}$). As a consequence, we need to reformulate δ as a function of the measurable parameters by SPIRIT given in Eq. (2). From Eq. (1) we get:

$$\delta^0\left(\left(^{13}C/^{12}C\right) \times \left(^{12}C/^{13}C\right)\text{VPDB}-1\right) \times 1000 \quad \text{for sampling air} \tag{2a}$$

$$\delta^0 = \left(\left(^{13}C^0/^{12}C^0\right) \times \left(^{12}C/^{13}C\right)\text{VPDB}-1\right) \times 1000 \quad \text{for } CO_2/\textit{air reference cylinder.} \tag{2b}$$

From Eqs. (2a) and (2b) we get Eq. (2c), where, δ is expressed directly from measured parameters in the field:

$$\delta = \left(\left(^{13}C/^{12}C\right) \times \left(^{12}C^0/^{13}C^0\right) \times \left(1 + \delta^0/1000\right)-1\right) \times 1000 \tag{2c}$$

where, δ^0 = −40.53‰ VPDB (C1) or −43.24‰ VPDB (C2) or −43.20‰ VPDB (C3).

1.2. *Performances of SPIRIT for $\delta^{13}C$ of CO_2 determination*

1.2.1. *Variance plots for $\delta^{13}C$ of CO_2*

The log–log plot of Allan variance (σ^2_{Allan}) (‰) of $\delta^{13}C$ *versus* integration time (Fig. 4) provides the time dependence of the precision and the possible drift behavior of the instrument, *i.e.*, the bias change over time. The minimum variance σ^2_{Allan} of 0.003‰ at 30 sec and variance of 0.02‰ at 1000 sec integration time, *i.e.*, σ_{Allan} of 0.05‰ and of 0.17‰ respectively, are given for low δ (−40.5‰) compressed synthetic air (Fig. 4a). Similar minimum variance σ^2_{Allan} of 0.007‰ at 30 sec and variance of 0.02‰ at 1000 sec integration time, *i.e.*, σ_{Allan} of 0.08‰ and of 0.14‰ respectively, are given for high δ (−10.2‰) compressed room air (Fig. 4b). The minimum variance value describes the turn-over point where the random noise becomes dominated by additional drift noise, likely due to temperature drift of the optical absorption cell. σ_{Allan} of 0.2‰ for 20 min integration time is similar to the bias drift of the reference cylinder observed under field conditions 20 min after calibration, where air sample is analyzed between calibration and drift measurement. The log–log plot of Allan variance (σ^2_{Allan}) (‰) of $\delta^{18}O$ *versus* integration time is also displayed in Fig. 4, as no calibration is needed to get this information. Similar minimum variance at 30 sec integration time is observed.

1.2.2. *$\delta^{13}C$ of CO_2 precision and accuracy for the scale range of δ encountered during the investigation of biogeochemical processes*

Tables 1 and 2 provide the precision of SPIRIT on $\delta^{13}C$ of CO_2 at values close to −43‰ and −10‰, representative of the δ range encountered from different sources of CO_2 produced from biogeochemical processes (Aggarwal and Hinchee, 1991; Boutton, 1991). In Tables 1 and 2, compressed synthetic air (20 L, 200 bar) certified in mixing ratio (390.0 ppmV) and analyzed in isotopic composition (δ^0 = −43.24‰ ± 0.28‰ VPDB) is used to calibrate SPIRIT.

SPIRIT is only calibrated with the δ^0 value of −43.24‰ VPDB according to Eq. (2c) above. As a consequence, the quality of SPIRIT measurements for the upper values of δ needs to be estimated from ambient/room air tanks also measured in isotopic signature by gas bench-IRMS (~−10‰ VPDB). In Table 1, SPIRIT is first calibrated with the δ^0 compressed synthetic air during 3 min and then the upper δ is measured for 3 min (10 replicates). As shown in Table 1, δ values for ambient pressure air and compressed room air measured with SPIRIT (−10.90‰ ± 0.31‰ and −10.18‰ ± 0.55‰ VPDB) agree with the ones measured by gas bench IRMS values (−10.64‰ ± 0.13‰ and −10.25‰ ± 0.07‰ VPDB), respectively. Thus, no significant

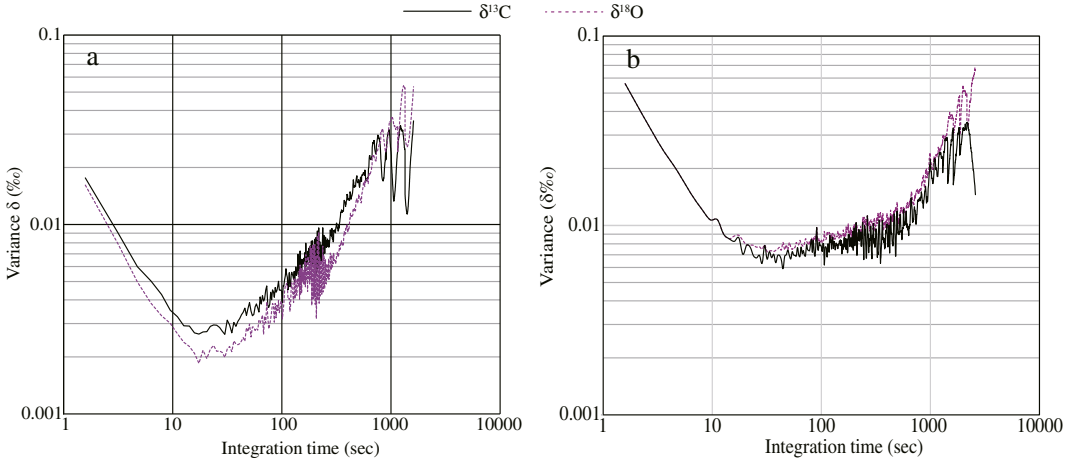

Fig. 4 – Allan variance (σ^2_{Allan}) of $\delta^{13}C$ values and $\delta^{18}O$ values *versus* integration time (a) from compressed synthetic air cylinder labeled C1 (CO_2 407 ppmV; $\delta^{13}C$ −40.53‰ VPDB) and (b) from compressed room air cylinder (CO_2 378 ppmV; $\delta^{13}C$ −10.18‰ VPDB). VPDB: Vienna Pee Dee Belemnite; $\delta^{13}C$ and $\delta^{18}O$ refer to isotopic signature ^{13}C and ^{18}O of CO_2, respectively.

Table 1 – Calibration of SPIRIT with certified compressed synthetic air and comparison with high δ values using atmospheric air.

Monitored parameter	X (ppmV)	δ (‰)	σ_δ (‰)	X (ppmV)	σ_X (ppmV)	δ (‰)	σ_δ (‰)
Compressed synthetic air labeled C2 (20 L, 200 bar)	390 [a]	−43.24 [a]	0.28 [a]	390.0 [b]	0.16 [(c)]	−43.24 [b]	0.30 [c]
Ambient pressure room air	NA	−10.64 [a]	0.13 [a]	384.3 [d]	0.47 [d]	−10.90 [d]	0.31 [d]
Compressed room air (10 L, 100 bar)	NA	−10.25 [a]	0.07 [a]	378.0 [d]	0.24 [d]	−10.18 [d]	0.55 [d]
Type of certification	Air Liquide®	IRMS	IRMS	SPIRIT	SPIRIT	SPIRIT	SPIRIT

X: CO_2 volume mixing ratio; δ: isotopic signature ^{13}C of CO_2; σ_δ and σ_X: standard deviation of δ and X; NA: not applicable; IRMS: isotope ratio mass spectrometry; SPIRIT: spectrometer infra-red *in situ* tropospheric.

[a] Certified values of X (from Air Liquide Industry) and certified values of δ and σ_δ (from analysis performed at Bureau de Recherches Géologiques et Minières by gas bench IRMS).

[b] Reference used to calibrate SPIRIT.

[c] Precision given for 3 min data analysis (10 replicates averaged).

[d] SPIRIT is first calibrated with the δ^0 compressed synthetic air during 3 min and then the upper δ is measured for 3 min (10 replicates) with ambient pressure or compressed room air.

bias is observed for the upper values of $\delta^{13}C$ of CO_2. The bias value of the $\delta^{13}C$ of CO_2 measured by SPIRIT relative to IRMS is on average lower than 0.2‰ for these high (~−10‰) isotopic reference cylinders, as shown here, and is similar for the low (~−43‰) isotopic reference cylinders. This 0.2‰ bias value can be also considered as the accuracy of SPIRIT relative to IRMS.

In Table 2, the precision of SPIRIT on $\delta^{13}C$ of CO_2 *versus* time delay, at values close to −43‰, is estimated under similar time series used in the field to determine the isotopic signature of a CO_2 source at the land–air interface (see next section for the field protocol). δ precision (‰) is calculated by the standard deviation σ of compressed synthetic and ambient air, according to the protocol given in Table 2, *i.e.*, calibration of SPIRIT with compressed synthetic air (20 L, 200 bar) during 3 min; measurement of ambient air during 10 min, drift analysis after measurement with the compressed synthetic air during 3 min. Table 2 shows a δ precision for sampled gas of about 0.4‰, with no significant drift after 10 min of measurements, which is a representative period (3 to 30 min) for CO_2 analysis emissions at ground surface from contaminated aquifers (see next section).

The closed chamber method is also used to check the linearity of some variables *versus* others to identify potential bias of the instrument. Serial injections of high CO_2 concentration (10% volume mixing ratio in dry air) is performed using a small volume (10 mL) gas chromatography (GC) syringe relative to the large 15 L volume chamber, starting from air zero (without H_2O, CO_2 and volatile organic compounds) inside the chamber. Linear increase of CO_2 mixing ratio (~65 ppm/injection) *versus* injection number is observed up to 1500 ppm. The best linear increase is found from 300 to 900 ppm (with a squared correlation coefficient $R^2 > 0.998$). Also, δ is found to be −33.4‰ ± 0.3‰ with no significant δ dependence (≤0.4‰) as a function of CO_2 mixing ratio, as it should be expected. Similar insignificant δ dependence is also observed for the upper values of δ (+4‰) by degassing CO_2 inside the chamber from the reaction of commercial clay with concentrated hydrochloric acid.

1.2.3. Precision and accuracy for $\delta^{13}C$ of CO_2 using the closed chamber method and the Keeling plot approach in field implementation

Fluxes and $\delta^{13}C$ of CO_2 emission are derived from the closed chamber method as described in Guimbaud et al. (2011). The optical cell of SPIRIT is connected to the top of the 15 L and 31 cm height CO_2 accumulation chamber. The latter one is set on a permanent polyvinylchloride (PVC) cylinder collar (30 cm diameter and height) sunk 15 cm into the soil. Air is sampled from and re-injected to the chamber via two PFA Teflon tubes (3 or 15 m length; 6 mm external diameters) protected from an external water proof larger tube. Sampling flow rate is typically 1 standard L/min through the PFA tubes and the SPIRIT optical cell. The top 15 cm soil layer has been removed before the PVC collar installation to avoid additional sources of CO_2 emission such as surface biomass respiration, in order to monitor in vast majority CO_2 emissions from biodegradation of the fuel leak.

The flux of CO_2 is calculated from the slope of the stabilized linear increase of the CO_2 mixing ratio with time, recorded during 5 min. The flux of CO_2 per surface unit (molecules/(m^2·sec)) is defined as F^S:

$$F^S = P \times h/(k_B \times T) \times (dX/dt) \quad (3)$$

Table 2 – Precision on δ using certified compressed synthetic air and compressed room air, where a 10 min period is representative for CO_2 analysis emissions at ground surface from contaminated aquifers.

Monitored parameter	X (ppmV)	σ_X (ppmV)	δ (‰)	σ_δ (‰)	Protocol (10 replicates)
Compressed synthetic air (20 L, 200 bar)	389.9[a]	0.176 [a]	−43.32 [a]	0.37 [a]	Calibration (3 min)
Compressed room air (10 L, 100 bar)	378.0	0.236	−10.18	0.43	Measurement (10 min)
Compressed synthetic air (20 L, 200 bar)	390.1[b]	0.229 [b]	−42.94 [b]	0.41 [b]	Drift analysis (3 min)

The reference synthetic compressed CO_2/air cylinder labeled C2 (X^0 = 390 ppmV and δ^0 = −43.24‰ ± 0.28‰ VPDB) is used.

VPDB: Vienna Pee Dee Belemnite.

[a] Values recalculated during calibration.

[b] Values from drift analysis 10 min later.

where, P (Pa) is pressure inside the chamber, k_B (J/K) is Boltzmann constant, T (K) is absolute temperature inside the chamber, h (m) is mean height of the chamber above soil surface, X (unit-less) is volume mixing ratio of CO_2, dX/dt (sec^{-1}) is rate of accumulation of CO_2.

The $\delta^{13}C$ signature of the emitted CO_2 is given by the Y intercept derived from the linear regression of $\delta^{13}C$ of CO_2 *versus* $1/CO_2$ mixing ratio measured inside the accumulation chamber, defined as Keeling plot method (Pataki et al., 2003) as developed below and given by the final Eq. (4e).

This result is obtained by mass balance conservation equations applied for isotope concentration $^{12}C + {}^{13}C = C$ (Eq. (4a)) and ^{13}C (Eqs. (4b) and (4c)),

$$C^{Ch} = C^A + C^S \tag{4a}$$

$$^{13}C^{Ch} = {}^{13}C^A + {}^{13}C^S \tag{4b}$$

$$C^{Ch} \times R^{Ch} = C^A \times R^A + C^S \times R^S \tag{4c}$$

where, C^{Ch}, C^A and C^S are defined as CO_2 volume mixing ratios in the accumulation chamber, in the outside air (initially present inside the chamber) and from the emission source; R^{Ch}, R^A, R^S, δ^{Ch}, δ^A and δ^S are the respective isotopic ratios (R) and isotopic signature (δ) of $^{13}C/^{12}C$ of CO_2 (‰ VPDB).

Dividing Eq. (4c) by R_{VPDB} and then substituting the resulting equation by Eq. (4a) we get:

$$C^{Ch} \times \delta^{Ch} = C^A \times \delta^A + C^S \times \delta^S. \tag{4d}$$

From Eq. (4a):

$$C^S = C^{Ch} - C^A$$

and if this equation is injected into Eq. (4d) it gives:

$$C^{Ch} \times \delta^{Ch} = C^A \times \delta^A + \left(C^{Ch} - C^A\right) \times \delta^S$$

and

$$\delta^{Ch} = C^A\left(\delta^A - \delta^S\right)\left(1/C^{Ch}\right) + \delta^S. \tag{4e}$$

CO_2 accumulation in the closed chamber starts at ambient air CO_2 concentration (around 390 ppmV) to reach 1000 ppmV for an accurate determination of the $\delta^{13}C$ for the emitted CO_2 (δ^S). The delay of accumulation lasts from several minutes to 1 hr depending on the emission rate of CO_2. The intercept precision, obtained from the linear regression of δ^{Ch} *versus* $1/C^{Ch}$, is typically 0.1‰ for δ^S value.

Gas bench IRMS isotopic signature is derived with a precision or reproducibility of 0.11‰ for 10 bulb samples and with an analytical accuracy (bias) <0.3‰. In the field, calibrations are performed during 3 min each time before isotopic signature measurements of CO_2 emissions. CO_2 accumulation usually lasts no longer than 40 min to avoid a $\delta^{13}C$ time drift due to temperature change of the optical system. Drift analysis of $\delta^{13}C$ of calibration cylinder is checked just after 3 min integration time, just before calibration again. In addition, a reference compressed ambient/room air gas cylinder (δ^0 close to −10.2‰ VPDB) is used to regularly check $\delta^{13}C$ accuracy in the upper data range of possible isotopic signature obtained in the field.

All sequences to derive the flux and $\delta^{13}C$ of CO_2 emission from ground are presented in Fig. 5 for collar number 16 on 2 August, 2014. In Fig. 5a and b, sequence A is the calibration of SPIRIT performed during 3 min with the CO_2 gas standard cylinder C3 (406 ppmV and δ^0 = −43.20‰ VPDB); sequence B is ambient air analysis (385 ppmV and δ = −11.5‰ VPDB) during 3 min where the chamber is lifted up to 1 m above ground, to flush the optical cell from calibration gas after the electronic valve switch; sequence C is flux emission measurement from ground during 5 min (for this collar) where the chamber is set on the collar until 1000 ppmV of CO_2 is reached inside the closed chamber (in Fig. 5a, the flux is given by the slope of the linear mixing ratio rise); sequence D is a repetition of sequence B; and sequence E is a 3 min analysis of the CO_2 gas standard cylinder for time drift analysis. From sequence C in Fig. 5b, δ values are used to obtain the Keeling plot in Fig. 5c. The isotopic signature of the CO_2 emission source is given by the Y axis origin intercept (δ^S = −30.7‰ VPDB) derived from linear regression in Fig. 5c.

Precision for δ^S, derived on the field from a single Keeling plot, is <0.43‰. δ^S precision (random error) is given by the root of the sum of the square of each maximum individual precision involved to reach its value, *i.e.*, 0.11‰ for gas bench-IRMS, 0.4‰ for SPIRIT drift analysis after 20 min of Keeling plot analysis, and 0.1‰ for the Keeling plot intercept. δ^S accuracy (bias) of 0.32‰ is also given by the root mean error method propagation taking into account the accuracy provided by the gas bench-IRMS (0.3‰), used as the reference for the absolute calibration of SPIRIT and the accuracy of the absorption ratio for the 2 isotopes equivalent to the isotope concentration ratio $^{13}C/^{12}C$ (0.1‰). Therefore, the overall uncertainty for δ^S, derived from one Keeling plot on field deployment is in the order of 0.5‰ (0.53‰ calculated for 20 min of accumulation).

2. Ground surface gas analysis method for monitoring aerobic bio-remediation of a BTEX-polluted site in SPIRIT field implementation

In situ monitoring of hydrocarbon contaminated aquifers treated through biodegradation is often expensive, intrusive and technically challenging. Conventional intrusive groundwater sampling campaigns need the installation of costly monitoring wells for vertical profile analysis restricted at some discrete locations only. As a consequence, data collected could not provide the most relevant information because significant subsurface heterogeneity exists with regard to hydrocarbon distribution in contaminated aquifers, soil texture and permeability.

To overcome these limitations and to reduce the cost of the monitoring, two new alternative surface analysis methods have been tested simultaneously at a benzene–toluene–ethylbenzene–xylenes (BTEX)-polluted site under aerobic bio-treatment within a project named BIOPHY (optimization of biodecontamination processes of contaminated aquifers with hydrocarbons by on-line geophysical and gas analysis monitoring) funded by the French National Agency for Research (ANR ECOTECH, 2010): geophysical methods (electrical resistivity and induced polarization) and gas flux

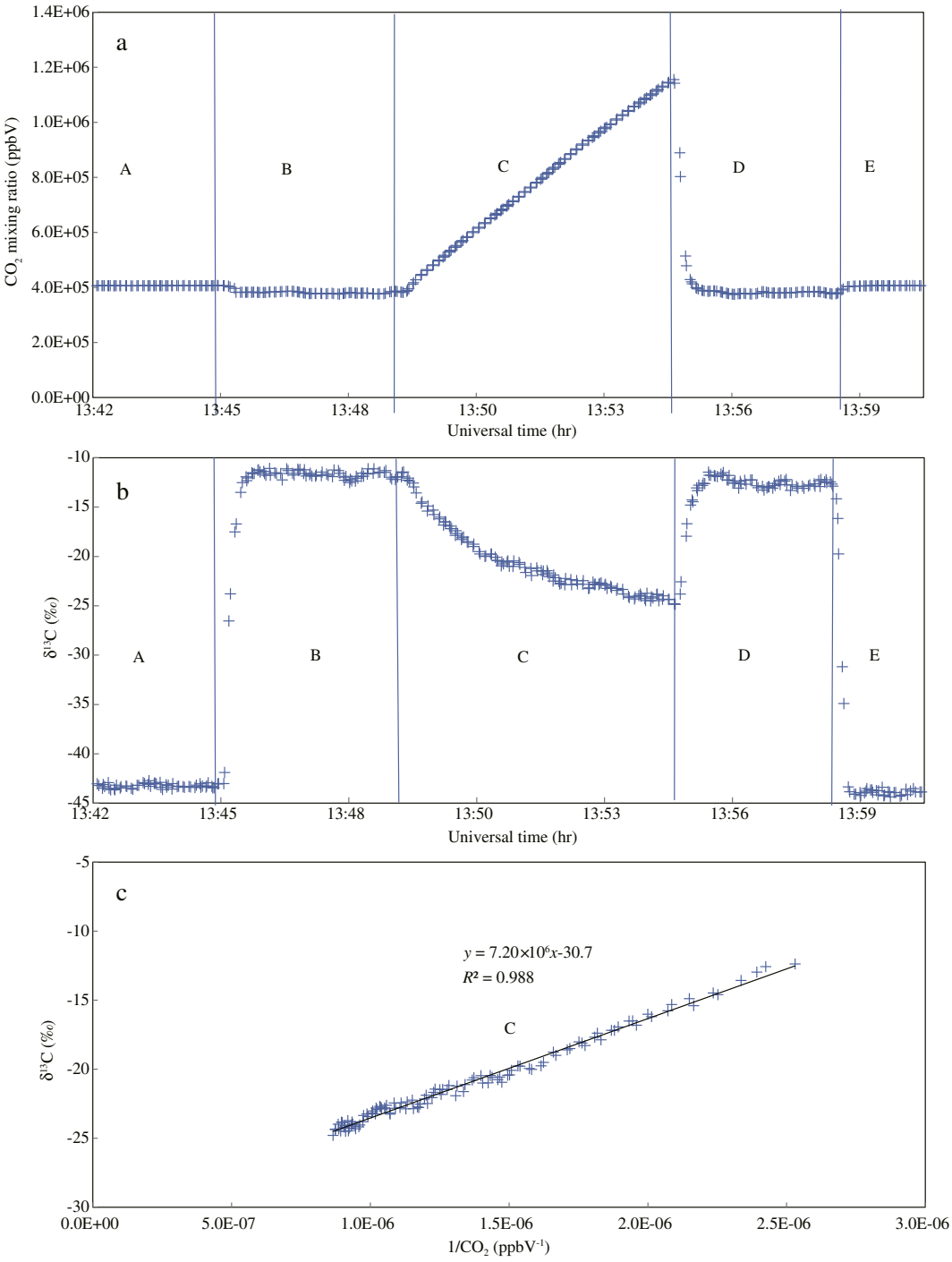

Fig. 5 – (a) CO_2 mixing ratio and (b) $\delta^{13}C$ *versus* universal time (UT) and (c) $\delta^{13}C$ *versus* $1/CO_2$ during sequence C for collar number 16 at 13:49 UT on 2 August 2014. Sequence A: calibration with standard cylinder labeled C3 (CO_2 406 ppmV; $\delta^{13}C$ –43.20‰ VPDB); sequences B and D: ambient air analysis; C: flux measurement from collar; E: same as A for drift analysis.

measurement method (CO_2 emissions at ground surface with isotopic concentration ratio $^{13}C/^{12}C$ determination). Geophysical methods and the combination with the gas analysis method are widely discussed in Noel et al. (2016a,b). The aim of the present paper is to demonstrate that a gas analysis method at ground surface could be promising to provide a new methodology for *in situ* monitoring at the level of the current performances of SPIRIT.

2.1. State of the art CO_2 as a tracer for biodegradation of hydrocarbons

During hydrocarbon biodegradation, there is production and emission of CO_2 (Kaufmann et al., 2004), and even carbon isotopic fractionation. Indeed, molecules with lighter isotopes ^{12}C could be preferentially degraded by bacteria (Meckenstock et al., 2004). Thus gas phase-released CO_2 will be enriched in

^{12}C with a weaker $\delta^{13}C$ than its initial, whereas residual pollutants will be depleted in ^{12}C with a higher $\delta^{13}C$.

Laboratory experiments using pure cultures of bacteria show that aerobic BTEX biodegradation can be accompanied by significant carbon isotope fractionation, with ^{13}C enrichment factors (ε values) of residual pollutant. For example Fischer et al. (2008) reported carbon enrichment factors of benzene between 0.7‰ and 4.3‰, and Morasch et al. (2002) found enrichment factor between 0.4‰ and 3.3‰ for toluene.

Water samples in hydrocarbon contaminated aquifers have shown similar enrichments of BTEX, *i.e.*, 3.8‰ for benzene, 2.6‰ for toluene, 1.3‰ for ethyl-benzene and 4.6‰ for xylene (Morasch et al., 2002), and 3.3‰ for benzene and 3.6‰ for naphthalene (Griebler et al., 2004).

Few analysis of CO_2 fractionation has been performed under well-defined bacteria environments. Jackson and Pardue (1999) have shown that aerobic biodegradation of hexadecane lead to no fractionation of CO_2 produced, whereas a negative fractionation of 5.6‰ can be measured for phenol (Hall et al., 1999). *In situ* experiments are often performed by CO_2 extraction from soils pumped from syringes, with a post analysis in laboratory using IRMS. As an example, Aggarwal and Hinchee (1991) investigated aerobic biodegradation in different locations contaminated by spilled or leaked jet fuel from air force base. CO_2 concentrations in soil gases varied from 0.2% VPDB to 2.2% VPDB in uncontaminated zones and from 0.6% VPDB to 13.0% VPDB in contaminated zones of the different locations. CO_2 in soil gases at uncontaminated zones displayed isotopic signature from plant root respiration and from decaying organic matter during the growing season which agrees with the photosynthesis pathway of carbon fixation of the vegetation type, *i.e.*, $\delta^{13}C$ of CO_2 ~−25‰ VPDB in temperate climates for plants using the C-3 cycle of carbon fixation and ~−12‰ VPDB in subtropical and desert climates for plants using the Hatch–Slack or C-4 cycle of carbon fixation. It is observed that $\delta^{13}C$ of CO_2 is more negative by 5‰ in all contaminated locations, indicating that the major part of CO_2 stored at the ground surface is accumulated from natural biodegradation of petroleum hydrocarbons which have very negative isotopic signature compared to surface organic matter. However, Aggarwal and Hinchee experiments do not provide quantification of hydrocarbon biodegradation rate from CO_2 analysis and still remain offline information. As a consequence, an online CO_2 flux measurement method at the scale of the contaminated zone with CO_2 origin quantification is needed to estimate the kinetic of a biodegradation process.

According to our knowledge, no investigation of CO_2 emission with isotopic signature determination has been performed from direct natural flux measurement at the soil–air interface with the aim to quantify natural flux losses of CO_2 from biodegradation covering an overall surface of an aquifer contamination zone from petroleum hydrocarbons within a large period of a biodegradation process, occurring often at the year scale.

2.2. Site

The field site studied is a gasoline station in France where gasoline and diesel fuels leaked in 1997 (Fig. 6). It is still in activity but the former tank installation (source of contamination) was dismantled. Several boreholes had been drilled for previous studies on this site. These studies showed that:

(1) the ground is mainly composed with silts and clays;
(2) it has a low permeability (between 10^{-6} and 10^{-7} m/sec);
(3) the direction of flow of the groundwater is from southeast to northwest;
(4) groundwater velocity is around 17 m/year;
(5) the water table level varies from 2.5 to 4.5 m depth;
(6) there is a significant amount of hydrocarbons such as BTEX in the area of the former tank installation due to the slow biodegradation rate of such aromatic compounds; and
(7) natural attenuation occurred in that site. Indeed, the presence of a bacterial flora is indicated by the absence of dissolved oxygen that matches the BTEX plume in water (Verardo et al., 2013).

As a natural biodegradation of hydrocarbons was already in process, a bio-treatment by an oxygen supply to stimulate aerobic biodegradation has been undertaken. A permeable reactive barrier was implemented to stop the plume migration. Biodegradation stimulation started on 27 March, 2014. Diluted H_2O_2 is added continuously to pumped water from the barrier. Then, oxygenated pumped water is injected below water table upstream the barrier.

Before bio-treatment, 21 PVC cylinder collars (diameter 30 cm) have been sunk into the soil allowing to cover CO_2 emissions all over the contaminated site (upstream, above and downstream the reactive barrier), as shown in Fig. 6. Measurements are performed every one or two months since February 2014.

2.3. Results and discussion

CO_2 fluxes with δ isotopic signatures are presented from February to December 2014 (Figs. 7 and 8). Some BTEX concentrations and δ values are also presented for May and December 2014 (Figs. 9 and 10). CO_2 emission rates increase in all spots from February to July (Fig. 7 and Table 3) from about 200 to 1500 ppb/sec in average, followed by a slow decay down to 600 ppb/sec in December. It is found that CO_2 emission rates are correlated to the annual cycle of the soil temperature and anti-correlated with the water table level (Table 3), in agreement with stimulation factors of biodegradation efficiency (temperature, oxygenation of the biofilm when water table is lowering in summer). Higher CO_2 emissions are observed at the barrier level since the beginning of bio-stimulation on 27 March 2014 (Fig. 7). CO_2 maximum values of fluxes observed, *i.e.*, ~10 to 100 μmol/(m^2·sec) (~400 to 4000 ppb/sec) from February to July, match with the polluted zone defined by geochemical borehole analyses of BTEX concentration (Fig. 9) downstream the former tank installation. These CO_2 fluxes are much larger than the average emissions due to vegetal grassland soil respiration, which commonly varies from 1 to 5 μmol CO_2/(m^2·sec) from winter to summer (Raich and Tufekciogul, 2000). In this site, natural soil respiration has been reduced by removing the 15 cm top layer of the ground surface for each collar sunk into the soil. CO_2 fluxes from uncontaminated area vary from ~0.7 to 2.5 μmol/(m^2·sec) (*i.e.*, ~30 to 200 ppb/sec). As a consequence, CO_2 emissions in this site are largely coming from bacterial

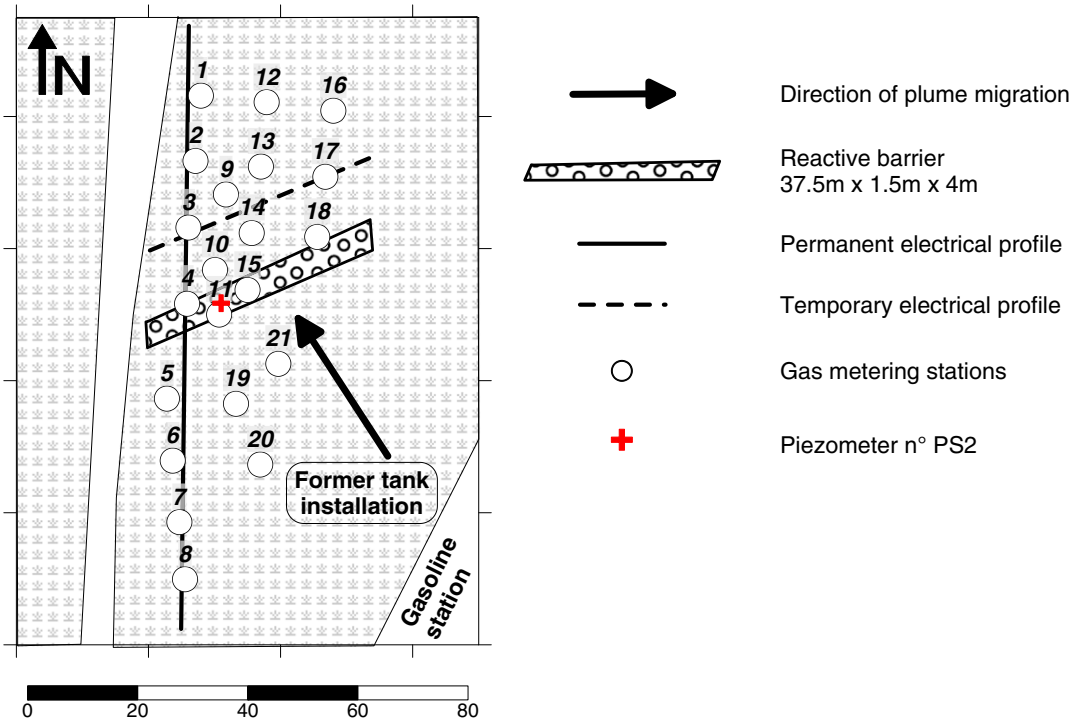

Fig. 6 – Map of the site showing the reactive barrier and the monitoring disposal. Each number (1–21) refers to a collar number for gas metering station.

respiration from biodegradation of hydrocarbons from the contaminated aquifer.

Precision on individual value obtained in the field for $\delta^{13}C$ of CO_2 from Keeling plot intercept after 5 to 60 min of CO_2 accumulation in chambers usually varies from 0.15‰ to 0.4‰ VPDB, respectively.

$\delta^{13}C$ of CO_2 time series (Fig. 8 and Table 3) leads to an average value of −28.3‰ VPDB from May to December with no significant change *versus* time. February data are not taken into account due to the large uncertainties existing in these data. One can note that the site is accessible two days per month (or per campaign) with a limited period (~6 hr) for effective measurements. Much weaker fluxes in February compared to the later periods induce a very long accumulation period for CO_2 in the chamber (20 to 60 min) to derive $\delta^{13}C$ of CO_2 from the Keeling method approach. As a consequence, less data points are available in February with lower precision due to larger drift of the instrument. Fluxes in July and October are strong enough to cover most of the plots of the site within this limited period. It can be observed that $\delta^{13}C$ of CO_2 emissions at ground surface in July varies from −30.5‰ ± 0.7‰ VPDB to −28.3‰ ± 1.6‰ VPDB from upstream to downstream the pollution plume (Fig. 8 and Table 4), corresponding to an increase of 2.2‰ VPDB; an increase of 1.1‰ VPDB remains in October. Same trends are observed for $\delta^{13}C$ of representative BTEX (benzene and toluene) in aquifer as shown in Fig. 10, despite the fact that they have not been measured at same periods, *i.e.*, earlier in May and later in December. Average evolution (May and December) of $\delta^{13}C$ of benzene and toluene in aquifer increases from −28.1‰ ± 0.5‰ VPDB to −26.7‰ ± 1.2‰ VPDB and from −27.4‰ ± 0.4‰ VPDB to −24.8‰ ± 1.9‰ VPDB, respectively, from upstream to downstream the pollution plume. These May and December $\delta^{13}C$ of CO_2 and of BTEX increases are mainly observed just few meters upstream the barrier (Fig. 11), indicating that biodegradation is mainly efficient after bioactivation. Results show that $\delta^{13}C$ of CO_2 released at the surface is lower than $\delta^{13}C$ of these two representative hydrocarbon sources with a difference of ~−2.5‰ VPDB upstream the barrier and of ~−4‰ VPDB downstream the barrier. This isotopic fractionation observed (~−3‰) through the stream of the pollution plume due to selection of light isotopes (^{12}C) from bacterial metabolism is in agreement with reporting data from authors in Section 2.1.

From July data (Table 4), it can be also noted that $\delta^{13}C$ of CO_2 measured directly from the water table (*i.e.*, measured directly through the PS2 piezometer labeled number PS2 in Fig. 6 between collars 10 and 15) is similar to the ones released through soil diffusion (*i.e.*, from collars). The four PS2 replicates $\delta^{13}C$ of CO_2 values (−30.0‰, −28.6‰, −28.8‰, −29.2‰ giving an average of −29.2‰ ± 0.6‰ VPDB) are similar to the two values given from the closest collars 10 and 15 (−30.3 and −29.5‰ VPDB) and to the averaged values upstream the bio-barrier 30.2‰ ± 0.9‰ VPDB. According to these data, no carbon isotopic fractionation of CO_2 occurs due to the transfer of CO_2 from its ground production to its land–air surface emission. Fractionation mentioned earlier is mainly due to bacterial metabolism discrimination.

Our data demonstrate that CO_2 flux can be correlated with biodegradation efficiency of hydrocarbons from the contaminated aquifer within the precision given from SPIRIT. Flux and $\delta^{13}C$ of the CO_2 released at the ground surface as well as $\delta^{13}C$ comparison with BTEX pollutants in aquifer show that

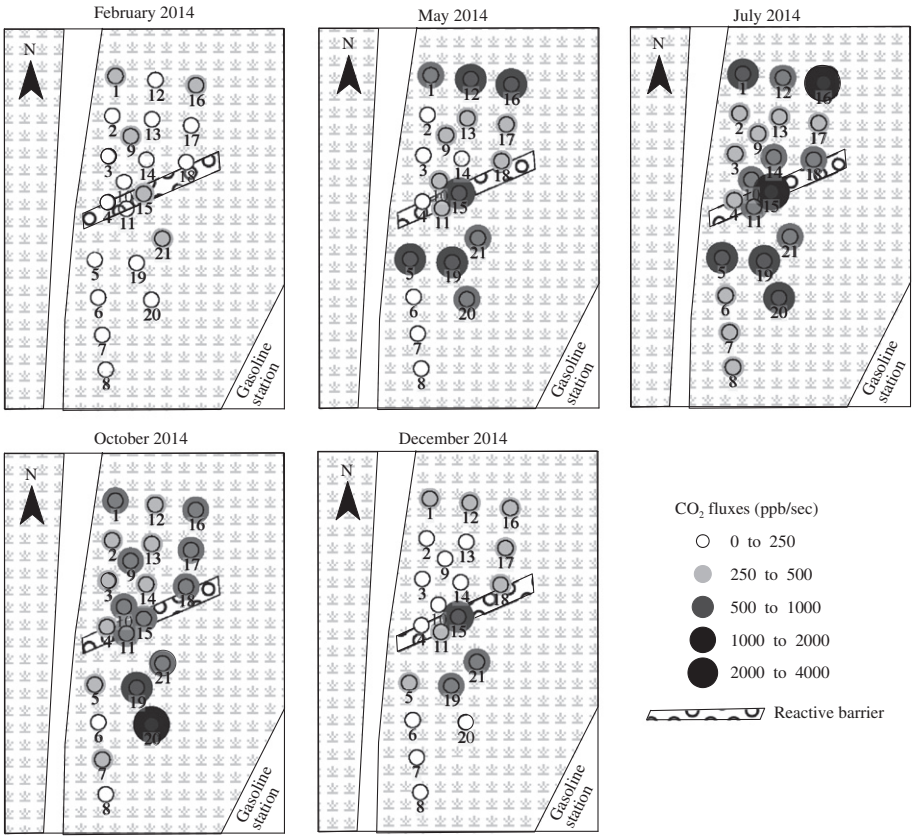

Fig. 7 – CO_2 flux time series. Each number (1–21) refers to a collar number for gas metering station.

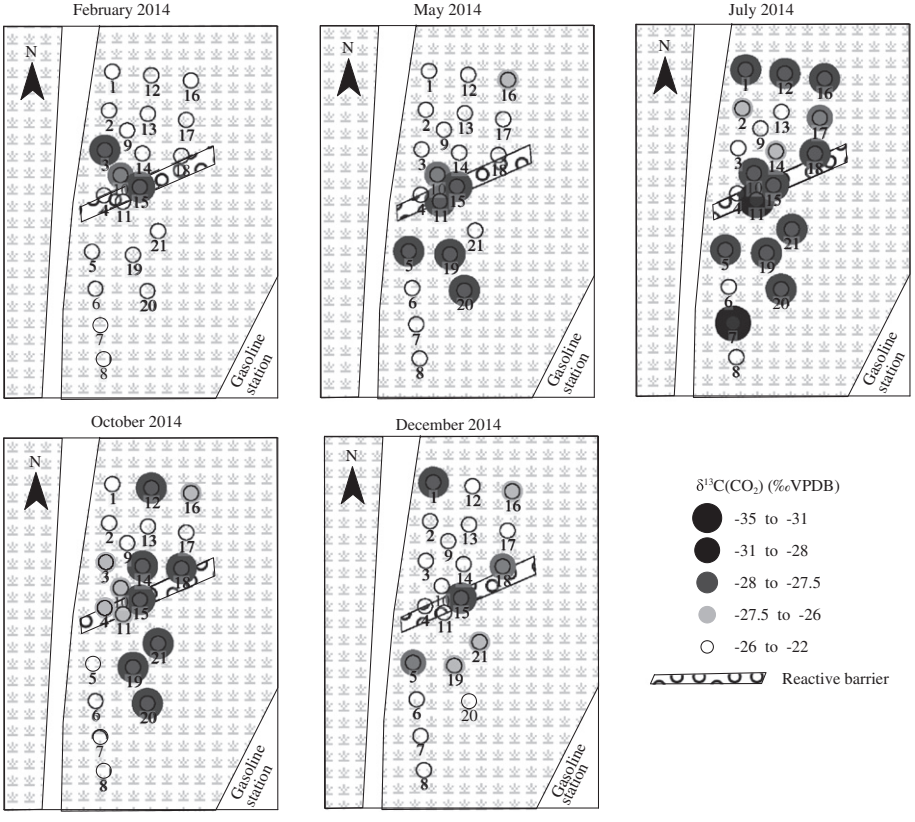

Fig. 8 – $\delta^{13}C$ values of CO_2 time series. Each number (1–21) refers to a collar number for gas metering station.

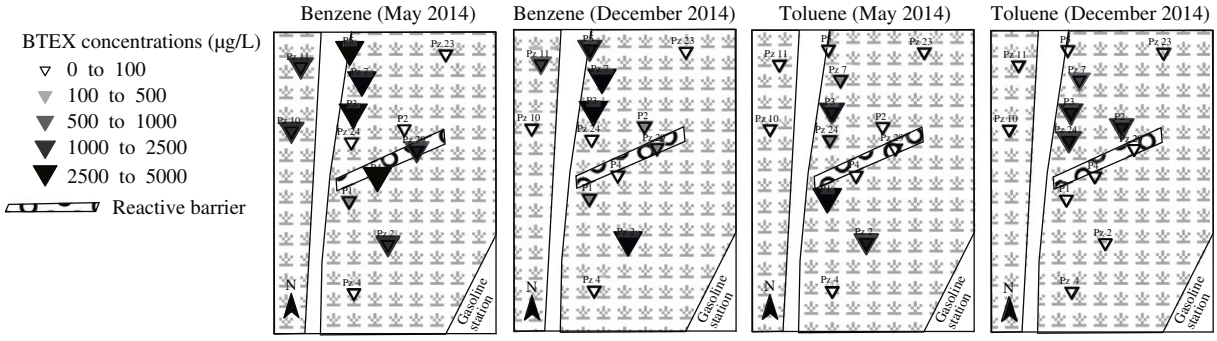

Fig. 9 – Benzene and toluene concentrations in aquifer. BETX: benzene–toluene–ethylbenzene–xylenes hydrocarbon family; P1–P5 and Pz 2–Pz 29 refer to piezometer number installed in the site (only piezometers where BTEX are sampled from water table are shown in the figure).

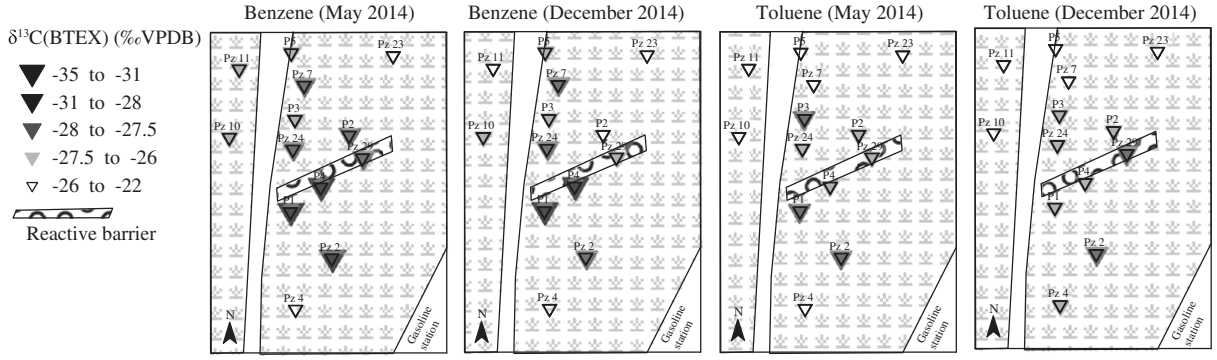

Fig. 10 – $\delta^{13}C$ values of benzene and toluene time series in aquifer.

CO_2 released into atmosphere is largely coming from biodegradation of the hydrocarbon polluted plume in that specific site. In such contaminated site, hydrocarbon degradation kinetic could be calculated and the efficiency of a depollution process evaluated. More investigation should be done using this method.

3. Summary and conclusion

An isotope ratio infra-red spectrometer (IRIS) has been developed to measure CO_2 flux with $\delta^{13}C$ isotopic signature of CO_2 with a precision better than 0.3‰, in addition to the measurement of fluxes of other greenhouse gases (CH_4, N_2O), thanks to the implementation of the SPIRIT instrument by the development of a new variable length path optical cell regulated in temperature with a precision of ±0.02°C. As an application, the new SPIRIT instrument has been tested on a BTEX-polluted site (gasoline station where gasoline and diesel fuels leaked) under aerobic bio-treatment to propose a non-intrusive method for monitoring *in situ* biodegradation of hydrocarbons. CO_2 flux measurements using the closed chamber method was combined with the determination of the isotopic signature $\delta^{13}C$ of the CO_2 emission using the Keeling plot method.

Table 3 – Average CO_2 flux and $\delta^{13}C$ values of CO_2 time series compared to other parameters in 2014.

Month	February	May	July	October	December
Chamber temperature (°C)	10.8	19.7	27.6	15.9	3.9
Soil temperature at ground surface (°C)	5.7	14.6	17.4	15.4	10.9
Water table temperature in piezometer number Pz 2 at −5.29 m (°C)	12.7	12.7	12.4	14.4	14.6
Water table depth in piezometer number P4 (m)	−1.59	−2.2	−2.44	−3.21	−3.03
Flux (ppbV/sec)[a]	190	700	1470	960	560
Flux (µmol/(m^2·sec))	42	155	331	214	125
$\delta^{13}C$ (‰ VPDB)	−25.4	−28.8	−29.3	−27.5	−27.7
σ (‰ VPDB)	4.1	2.5	1.4	1.2	1.4

$\delta^{13}C$: isotopic signature ^{13}C of CO_2; σ: standard deviation of $\delta^{13}C$; VPDB: Vienna Pee Dee Belemnite.
[a] Chamber mean high 61 cm.

Table 4 – Average $\delta^{13}C$ and flux of CO_2 relative to the barrier.

Monitored parameter	July			August		
	$\delta^{13}C \pm \sigma$ (‰ VPDB)	Flux (ppb/sec)	Number of collar	$\delta^{13}C \pm \sigma$ (‰ VPDB)	Flux (ppb/sec)	Number of collar
Downstream barrier (north)	−28.3 ± 1.6	1020	8	−27.0 ± 1.2	400	8
Upstream barrier (south)	−30.5 ± 0.7	1280	7	−28.1 ± 1.1	1600	5
Piezometer number PS2: located upstream collar 10	−29.2 ± 0.6	NA	4 replicates	NA	NA	NA

$\delta^{13}C$: isotopic signature ^{13}C of CO_2; VPDB: Vienna Pee Dee Belemnite.

On that specific site, SPIRIT instrument using IRIS technology has proven its sensitivity to demonstrate that CO_2 emissions from the contaminated soil are mainly originating from the biodegradation of the hydrocarbons from the pollution liquid plume: (i) CO_2 emissions match with the polluted zone defined by geochemical borehole analyses (BTEX and other hydrocarbon concentration) and (ii) isotopic signatures $\delta^{13}C$ of CO_2 emissions at ground surface are correlated with the $\delta^{13}C/^{12}C$ of the main hydrocarbons (benzene and toluene) present in aquifer from upstream to downstream the pollution plume with a fractionation that corresponds to bacterial metabolism for biodegradation of BTEX into CO_2.

From this work, it appears that ground surface gas analysis (CO_2 flux with isotopic signature determination) could be a non-intrusive method allowing for quantifying remediation kinetic of a gasoline contaminated soil on real time *in situ* at the scale of the polluted plume.

Indeed, such polluted sites from gasoline station are widespread in France and worldwide. Low cost methods to monitor soil depollution could be applied by continuous CO_2 flux measurements using automatic chambers and cheap CO_2 probes such as "©Vaisala probes" (GMP343 Carbon Dioxide Probe) (Vaisala Oyj, Helsinki, Finland) located at ground surface within an appropriate grid pattern to cover the pollution liquid plume. CO_2 biogeochemical origins can be quantified from isotopic signature $\delta^{13}C/^{12}C$ of the CO_2 monitoring by using IRIS portable instruments. Despite the fact that IRIS instrument operation still requires human presence on the site, human resource cost can be limited because $\delta^{13}C/^{12}C$ of the CO_2 measurements at the field only needs to be performed at discrete times to quantify CO_2 emission origin during a depollution process period.

In addition to be a non-intrusive method for *in situ* monitoring, remediation efficiency policy could be evaluated and decided in real time from ground surface gas analysis. Also, the best cost efficiency policy for the choice of the remediation process can be defined at an early stage (bio stimulation *versus* natural remediation; bio- or chemical depollution) as a function

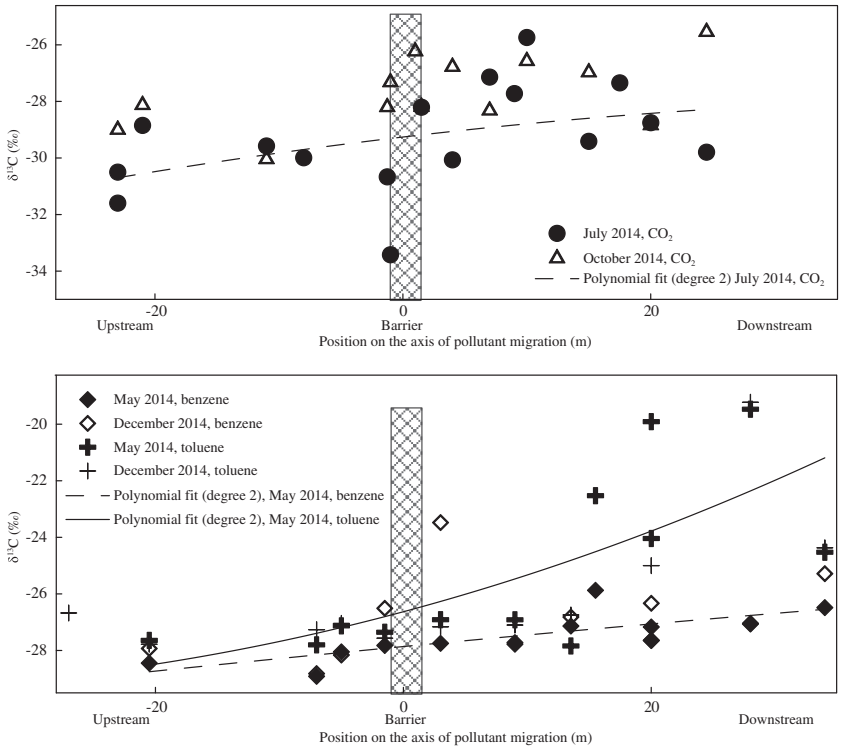

Fig. 11 – $\delta^{13}C$ values of benzene and toluene in aquifer and CO_2 emission at ground surface reported along the axis of the pollution plume.

of environmental risks (river or ground water contamination) or economic interests (deadlines for future land use or sells) to take into account, if relevant.

Acknowledgments

The paper is a contribution to the research conducted at OSUC (Observatoire des Sciences de l'Univers en Région Centre, Centre National de la Recherche Scientifique-Université Orléans) supported by the following projects of the French Research Agency: ECOTECH BIOPHY (Optimisation de procédés de BIOdépollution des eaux souterraines contaminées par des hydrocarbures par un monitoring géoPHYsique et analyse de gaz en ligne) (ANR-10-ECOT-014) and LABEX VOLTAIRE (LABoratoire d'EXcellence VOLatils — Terre, Atmosphère et Interactions — Ressources et Environnement) (ANR-10-LABX-100-01). This work is also supported by the AMIS (FAte and IMpact of AtmospherIc PollutantS) project funded by the European Union, under the Marie Curie Actions IRSES (International Research Staff Exchange Scheme), within the Seventh Framework Programme FP7-PEOPLE-2011-IRSES. We gratefully acknowledge the engineering and technical staffs of the LPC2E (Laboratoire de Physique et de Chimie de l'Environnement et de l'Espace) K. le Letty, G. Chalumeau, S. Chevrier, F. Savoie, T. Vincent, as well as master internship students P. Gaudry, S. Williams, G. Belot and post doctor C. Bahrini for their contribution to SPIRIT development or their participation in various field campaigns. We also thank all the partners of the BIOPHY project: Bureau de Recherches Géologiques et Minières (BRGM), SERPOL, TOTAL, who setup and managed the field study site for depollution by bio-stimulation, and E. Proust (BRGM) for IRMS calibration of reference cylinders.

REFERENCES

Aggarwal, P.K., Hinchee, R.E., 1991. Monitoring in situ biodegradation of hydrocarbons by using stable carbon isotopes. Environ. Sci. Technol. 25 (6), 1178–1180.

ANR ECOTECH, 2010. BIOPHY (2011–15): Optimisation de procédés de BIOdépollution des eaux souterraines contaminées par des hydrocarbures par un monitoring géoPHYsique et analyse de gaz en ligne; funded by the French National Agency for Research under theProgramme Production Durable et Technologies de l'Environnement". ANR-10-ECOT-014.

Boutton, T.W., 1991. Stable carbon isotope ratios of natural materials: II. Atmospheric, terrestrial, marine, and freshwater environments. In: Coleman, D.C., Fry, B. (Eds.), Carbon Isotope Techniques. Academic Press, New York, pp. 173–185.

Bowling, D.R., Burns, S.P., Conway, T.J., Monson, R.K., White, J.W.C., 2005. Extensive observations of CO_2 carbon isotope content in and above a high elevation subalpine forest. Glob. Biogeochem. Cycles 19 (3). http://dx.doi.org/10.1029/2004GB002394.

Craig, H., 1954. Carbon 13 in plants and the relationships between carbon 13 and carbon 14 variations in nature. J. Geol. 62 (2), 115–149.

Croizé, L., Mondelain, D., Camy-Peyret, C., Delmotte, M., Schmidt, M., 2008. Precise measurements of the total concentration of atmospheric CO_2 and $^{13}CO_2/^{12}CO_2$ isotopic ratio using a lead-salt laser diode spectrometer. Rev. Sci. Instrum. 79 (4). http://dx.doi.org/10.1063/1.2902829.

Ekblad, A., Högberg, P., 2000. Analysis of $\delta^{13}C$ of CO_2 distinguishes between microbial respiration of added C_4-sucrose and other soil respiration in a C_3-ecosystem. Plant Soil 219 (1–2), 197–209.

Fischer, A., Herklotz, I., Herrmann, S., Thullner, M., Weelink, S.A.B., Stams, A.J.M., et al., 2008. Combined carbon and hydrogen isotope fractionation investigations for elucidating benzene biodegradation pathways. Environ. Sci. Technol. 42 (12), 4356–4363.

Ghosh, P., Brand, W.A., 2003. Stable isotope ratio mass spectrometry in global climate change research. Int. J. Mass Spectrom. 228 (1), 1–33.

Gilbert, A., Silvestre, V., Segebarth, N., Tcherkez, G., Guillou, C., Robins, R.J., et al., 2011. The intramolecular ^{13}C-distribution in ethanol reveals the influence of the CO_2-fixation pathway and environmental conditions on the site-specific ^{13}C variation in glucose. Plant Cell Environ. 34 (7), 1104–1112.

Gogo, S., Guimbaud, C., Laggoun-Défarge, F., Catoire, V., Robert, C., 2011. In situ quantification of CH_4 bubbling events from a peat soil using a new infrared laser spectrometer. J. Soils Sediments 11 (4), 545–551.

Griebler, C., Safinowski, M., Vieth, A., Richnow, H.H., Meckenstock, R.U., 2004. Combined application of stable carbon isotope analysis and specific metabolites determination for assessing in situ degradation of aromatic hydrocarbons in a tar oil-contaminated aquifer. Environ. Sci. Technol. 38 (2), 617–631.

Grossel, A., Nicoullaud, B., Bourennane, H., Rochette, P., Guimbaud, C., Chartier, M., et al., 2014. Simulating the spatial variability of nitrous oxide emission from cropped soils at the within-field scale using the NOE model. Ecol. Model. 288, 155–165.

Guimbaud, C., Catoire, V., Gogo, S., Robert, C., Chartier, M., Laggoun-Défarge, F., et al., 2011. A portable infrared laser spectrometer for flux measurements of trace gases at the geosphere–atmosphere interface. Meas. Sci. Technol. 22 (7), 1–17.

Hall, J.A., Kalin, R.M., Larkin, M.J., Allen, C.C.R., Harper, D.B., 1999. Variation in stable carbon isotope fractionation during aerobic degradation of phenol and benzoate by contaminant degrading bacteria. Org. Geochem. 30 (8), 801–811.

Hornibrook, E.R.C., Bowes, H.L., 2007. Trophic status impacts both the magnitude and stable carbon isotope composition of methane flux from peatlands. Geophys. Res. Lett. 34 (21). http://dx.doi.org/10.1029/2007GL031231.

Jackson, A., Pardue, J., 1999. Quantifying the mineralization of contaminants using stable carbon isotope ratios. Org. Geochem. 30 (8), 787–792.

Kaufmann, K., Christophersen, M., Buttler, A., Harms, H., Höhener, P., 2004. Microbial community response to petroleum hydrocarbon contamination in the unsaturated zone at the experimental field site Værløse, Denmark. FEMS Microbiol. Ecol. 48 (3), 387–399.

Meckenstock, R.U., Morasch, B., Griebler, C., Richnow, H.H., 2004. Stable isotope fractionation analysis as a tool to monitor biodegradation in contaminated aquifers. J. Contam. Hydrol. 75 (3–4), 215–255.

Morasch, B., Richnow, H.H., Schink, B., Vieth, A., Meckenstock, R.U., 2002. Carbon and hydrogen stable isotope fractionation during aerobic bacterial degradation of aromatic hydrocarbons. Appl. Environ. Microbiol. 68 (10), 5191–5194.

Nelson, D.D., McManus, J.B., Herndon, S.C., Zahniser, M.S., Tuzson, B., Emmenegger, L., 2008. New method for isotopic ratio measurements of atmospheric carbon dioxide using a 4.3 μm pulsed quantum cascade laser. Appl. Phys. B90 (2), 301–309.

Noel, C., Gourry, J.C., Deparis, J., Ignatiadis, I., Battaglia-Brunet, F., Guimbaud, C., 2016a. Suitable Real Time Monitoring of the Aerobic Biodegradation of Toluene in Contaminated Sand by

Spectral Induced Polarization Measurements and CO_2 Analyses. Near Surf. Geophys. (accepted for publication).
Noel, C., Gourry, J.C., Deparis, J., Blessing, M., Ignatiadis, I., Guimbaud, C., 2016b. Combining geoelectrical measurements and CO_2 analyses to monitor the enhanced bioremediation of hydrocarbon-contaminated soils: a field implementation. Appl. Environ. Soil Sci., 869869
Pataki, D.E., Ehleringer, J.R., Flanagan, L.B., Yakir, D., Bowling, D.R., Still, C.J., et al., 2003. The application and interpretation of Keeling plots in terrestrial carbon cycle research. Glob. Biogeochem. Cycles 17 (1). http://dx.doi.org/10.1029/2001GB001850.
Raich, J.W., Tufekciogul, A., 2000. Vegetation and soil respiration: correlations and controls. Biogeochemistry 48 (1), 71–90.
Richter, D., Wert, B.P., Fried, A., Weibring, P., Walega, J.G., White, J.W.C., et al., 2009. High-precision CO_2 isotopologue spectrometer with a difference-frequency-generation laser source. Opt. Lett. 34 (2), 172–174.
Robert, C., 2007. Simple, stable, and compact multiple-reflection optical cell for very long optical paths. Appl. Opt. 46 (22), 5408–5418.
Rothman, L.S., Jacquemarta, D., Barbe, A., Chris Benner, D., Birk, M., Brown, L.R., et al., 2005. The *HITRAN* 2004 molecular spectroscopic database. J. Quant. Spectrosc. Radiat. Transf. 96 (2), 139–204.
Rothman, L.S., Gordon, I.E., Barbe, A., Chris Benner, D., Bernath, P.F., Birk, M., et al., 2009. The *HITRAN* 2008 molecular spectroscopic database. J. Quant. Spectrosc. Radiat. Transf. 110 (9–10), 533–572.
Schaeffer, S.M., Miller, J.B., Vaughn, B.H., White, J.W.C., Bowling, D.R., 2008. Long-term field performance of a tunable diode laser absorption spectrometer for analysis of carbon isotopes of CO_2 in forest air. Atmos. Chem. Phys. 8 (3), 5263–5277.
Schweizer, M., Fear, J., Cadisch, G., 1999. Isotopic (^{13}C) fractionation during plant residue decomposition and its implications for soil organic matter studies. Rapid Commun. Mass Spectrom. 13 (13), 1284–1290.
Tsuji, K., Fujikawa, S., Yamada, K., Yoshida, N., Yamamoto, K., Kikugawa, T., 2006. Precise measurement of the $^{13}CH_4/^{12}CH_4$ ratio of diluted methane using a near-infrared laser absorption spectrometer. Sensors Actuators B114 (1), 326–333.
Verardo, E., Guerin, V., Colombano, S., Gourry, J.C., Blessing, M., Zornig, C., et al., 2013. Rapport ATTENA de phase 2 du projet BIOPHY, Étude réalisée pour le compte de l'ADEME: Document interne: Cas d'étude de gestion de site par atténuation naturelle – site 3. PROJET ATTENA – PHASE 2(Internal report).
Whiticar, M.J., 1999. Carbon and hydrogen isotope systematics of bacterial formation and oxidation of methane. Chem. Geol. 161 (1–3), 291–314.
Witinski, M.F., Sayres, D.S., Anderson, J.G., 2011. High precision methane isotopologue ratio measurements at ambient mixing ratios using integrated cavity output spectroscopy. Appl. Phys. B102 (2), 375–380.